Article

Developmental Cell

Spatially Resolved Genome-wide Transcriptional Profiling Identifies BMP Signaling as Essential Regulator of Zebrafish Cardiomyocyte Regeneration

Graphical Abstract

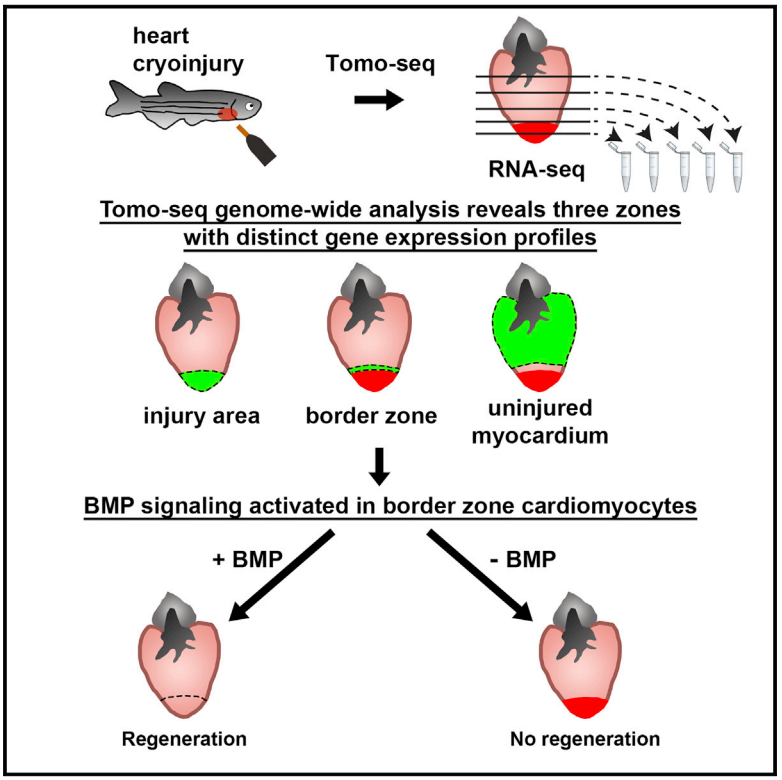

Authors

Chi-Chung Wu, Fabian Kruse, Mohankrishna Dalvoy Vasudevarao, ..., Alexander van Oudenaarden, Gilbert Weidinger, Jeroen Bakkers

Correspondence

gilbert.weidinger@uni-ulm.de (G.W.), j.bakkers@hubrecht.eu (J.B.)

In Brief

Wu, Kruse et al. apply tomo-seq, a technique for spatially resolved genome-wide transcriptional profiling, to the regenerating zebrafish heart. They identify BMP signaling as an essential regulator of zebrafish cardiomyocyte regeneration, via regulating injury-induced cardiomyocyte dedifferentiation and proliferation.

Highlights

- Tomo-seq reveals spatial gene expression profiles of regenerating zebrafish hearts
- The wound border zone expresses regulators and targets of BMP signaling
- BMP signaling is activated in cardiomyocytes and promotes their proliferation
- Heart regeneration requires BMP signaling and is enhanced by pathway activation

Accession Numbers

GSE74652

Wu et al., 2016, Developmental Cell *36*, 36–49
January 11, 2016
http://dx.doi.org/10.1016/j.devcel.2015.12.010

CellPress

CellPress

Developmental Cell
Article

Spatially Resolved Genome-wide Transcriptional Profiling Identifies BMP Signaling as Essential Regulator of Zebrafish Cardiomyocyte Regeneration

Chi-Chung Wu,[1,8] Fabian Kruse,[2,8] Mohankrishna Dalvoy Vasudevarao,[1] Jan Philipp Junker,[2] David C. Zebrowski,[3] Kristin Fischer,[4] Emily S. Noël,[2,10] Dominic Grün,[2] Eugene Berezikov,[5,6] Felix B. Engel,[3] Alexander van Oudenaarden,[2] Gilbert Weidinger,[1,9,*] and Jeroen Bakkers[2,7,9,*]

[1]Institute for Biochemistry and Molecular Biology, Ulm University, Albert-Einstein-Allee 11, 89081 Ulm, Germany
[2]Hubrecht Institute, University Medical Centre Utrecht, Uppsalaan 8, 3584 CT Utrecht, the Netherlands
[3]Experimental Renal and Cardiovascular Research, Department of Nephropathology, Institute of Pathology, Friedrich-Alexander-Universität Erlangen-Nürnberg (FAU), Krankenhausstr 8–10, 91054 Erlangen, Germany
[4]Institute of Clinical Genetics, Technische Universität Dresden, Fetscherstr. 74, 01307 Dresden, Germany
[5]European Research Institute for the Biology of Ageing, University Medical Center Groningen, University of Groningen, Antonius Deusinglaan 1, 9713 AV Groningen, the Netherlands
[6]Skolkovo Institute of Science and Technology (Skoltech), Novaya Street 100, Skolkovo, Moscow Region 143025, Russia
[7]Medical Physiology, University Medical Centre Utrecht, Yalelaan 50, 3584 CM Utrecht, the Netherlands
[8]Co-first author
[9]Co-senior author
[10]Present address: Bateson Center and Department of Biomedical Science, University of Sheffield, Firth Court, Western Bank, Sheffield S10 2TN, UK
*Correspondence: gilbert.weidinger@uni-ulm.de (G.W.), j.bakkers@hubrecht.eu (J.B.)
http://dx.doi.org/10.1016/j.devcel.2015.12.010

SUMMARY

In contrast to mammals, zebrafish regenerate heart injuries via proliferation of cardiomyocytes located near the wound border. To identify regulators of cardiomyocyte proliferation, we used spatially resolved RNA sequencing (tomo-seq) and generated a high-resolution genome-wide atlas of gene expression in the regenerating zebrafish heart. Interestingly, we identified two wound border zones with distinct expression profiles, including the re-expression of embryonic cardiac genes and targets of bone morphogenetic protein (BMP) signaling. Endogenous BMP signaling has been reported to be detrimental to mammalian cardiac repair. In contrast, we find that genetic or chemical inhibition of BMP signaling in zebrafish reduces cardiomyocyte dedifferentiation and proliferation, ultimately compromising myocardial regeneration, while *bmp2b* overexpression is sufficient to enhance it. Our results provide a resource for further studies on the molecular regulation of cardiac regeneration and reveal intriguing differential cellular responses of cardiomyocytes to a conserved signaling pathway in regenerative versus non-regenerative hearts.

INTRODUCTION

Myocardial infarction (MI) is a leading cause of death worldwide. In adult mammals, most cardiomyocytes lost after infarction are not replaced, and infarcted hearts develop permanent scars. In contrast, zebrafish display complete scar resolution and regeneration of lost cardiomyocytes after various insults, namely ventricular resection (Poss et al., 2002), genetic cardiomyocyte ablation (Wang et al., 2011), and cryoinjury-induced necrotic lesions (Chablais et al., 2011; Gonzalez-Rosa et al., 2011; Schnabel et al., 2011). Genetic fate-mapping experiments have revealed that zebrafish cardiomyocyte regeneration relies primarily on proliferation of spared cardiomyocytes, which show signs of dedifferentiation including disassembled sarcomeric structures and activation of regulatory sequences of the cardiac transcription factor *gata4* (Jopling et al., 2010; Kikuchi et al., 2010). While adult mammalian cardiomyocytes have long been considered to be post-mitotic, there is increasing evidence for low, yet significant cardiomyocyte turnover via proliferation in adult mammalian hearts (Bergmann et al., 2009; Senyo et al., 2013). Although the rate of natural adult cardiomyocyte proliferation is too low for effective cardiac repair in mammals, its discovery fosters the hope to heal hearts via therapeutic activation of endogenous cardiomyocyte proliferation. A thorough understanding of the mechanisms controlling cardiomyocyte regeneration in zebrafish will be instrumental in achieving this goal. While several signaling pathways have been implicated in zebrafish myocardial regeneration, including fibroblast growth factor, retinoic acid, transforming growth factor β (TGF-β), insulin-like growth factor, Jak1/Stat3, Notch, and Neuregulin signaling (reviewed in Gemberling et al., 2013, 2015), little is known about how these signaling pathways regulate cardiomyocyte replacement. Moreover, with the exception of the Jak1/Stat3 pathway (Fang et al., 2013), it is unclear whether these signals act cell-autonomously in cardiomyocytes or whether they are indirectly required for cardiomyocyte regeneration.

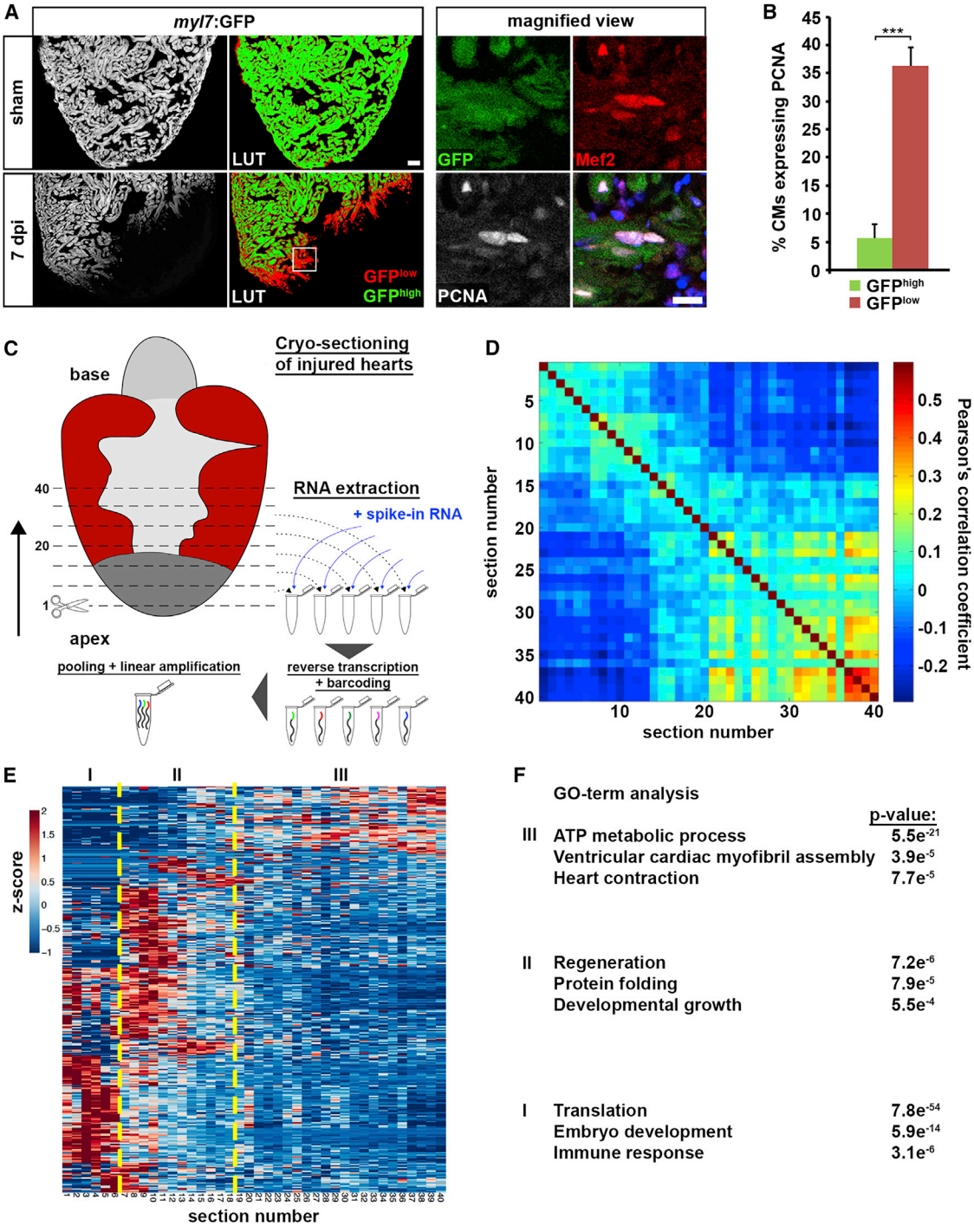

Figure 1. Tomo-Seq Identifies Genes with Spatially Restricted Expression in the Regenerating Heart

(A) Ventricular *myl7*:GFP expression is reduced at the wound border at 7 days post cryoinjury (dpi). In LUT (lookup table) images, GFP intensity below a threshold of 30% of signal intensity is displayed in red (GFP^{low}) while the rest is displayed in green (GFP^{high}). Boxed area is presented as magnified view,which shows examples of Mef2+, GFP^{low} cardiomyocytes expressing PCNA. Scale bars, 50 μm (overview) and 25 μm (magnified view).

(B) Average percentage of PCNA expressing GFP^{low} and GFP^{high} cardiomyocytes. Error bars represent SEM. Student's t test, ***p = 0.0003.

(C) Cartoon summarizing the tomo-seq procedure. Cryoinjured zebrafish ventricles were sectioned from apex to base. RNA from single sections was extracted, followed by reverse transcription and barcoding, after which the samples were pooled for linear amplification and sequence library preparation.

(D) Pairwise correlation between individual sections across all genes detected at more than four reads in more than one section of the 3 dpi heart.

(legend continued on next page)

BMP signaling plays several well-studied roles during vertebrate cardiovascular development (reviewed in van Wijk et al., 2007), while its role after cardiac injury is less clear. In mouse hearts BMP signaling appears to be activated within hours after MI, as indicated by expression of BMP ligands and accumulation of phosphorylated Smad1/5/8, a readout for active BMP signaling (Pachori et al., 2010). However, the cell types upregulating BMP signaling in response to injury have not been identified (Pachori et al., 2010; Zaidi et al., 2010). BMP gain-of-function experiments in vivo or in cardiomyocyte culture have revealed little about the endogenous function of BMP signaling in the injured mammalian heart, since several studies have reported contradictory results. BMP2 protein has been shown to induce cardiomyocyte cell-cycle re-entry in vitro and to reduce cardiomyocyte apoptosis both in vivo and in vitro (Chakraborty et al., 2013; Ebelt et al., 2013; Izumi et al., 2001), while BMP4 protein is able to enhance apoptosis and hypertrophy of cultured cardiomyocytes (Sun et al., 2013). Thus, it appears that exogenously supplied BMP ligands can elicit opposing responses in mammalian cardiomyocytes (Lu et al., 2014). On the other hand, loss-of-function data point toward a detrimental role for endogenous BMP signaling in the injured mammalian heart. Noggin binds to and blocks the function of several BMP ligands, with a preference for BMP2 and 4, but not the related TGF-β ligands (Zimmerman et al., 1996). In vivo treatment of mice with Noggin or the small-molecule BMP type-I receptor antagonist dorsomorphin reduces cardiomyocyte apoptosis as well as infarct size, and improves functional recovery after MI (Pachori et al., 2010). These results indicate that endogenous BMP signaling limits mammalian cardiomyocyte survival and regeneration.

Cellular injury responses occurring in cardiomyocytes at the wound border appear to be central for zebrafish heart regeneration. Further progress toward a mechanistic understanding of naturally occurring heart regeneration will thus be aided by a comprehensive view of molecular responses to injury in this border zone. To identify genes that are expressed in specific regions of a tissue of interest we developed tomo-seq, a method providing spatially resolved genome-wide expression profiles (Junker et al., 2014). Tomo-seq combines traditional histological techniques with low-input RNA sequencing to generate a high-resolution genome-wide atlas of spatially resolved gene expression. Importantly, tomo-seq data can be easily searched for genes that satisfy any desired spatial expression criteria.

Here we have applied tomo-seq to the regenerating zebrafish heart, which allowed us to identify genes enriched in the injury area, border zone, and uninjured myocardium. The border zone is characterized by the re-expression of embryonic cardiac genes, smooth muscle genes, and regulators of growth, such as BMP pathway genes. We found that BMP signaling is activated in border zone cardiomyocytes and that it is required for myocardial regeneration. Interestingly, the requirement of BMP signaling for cardiomyocyte proliferation appears to be regeneration specific, since it did not regulate physiological cardiomyocyte proliferation during cardiogenesis but was required for injury-specific cellular responses of cardiomyocytes, namely dedifferentiation and cell-cycle re-entry. Our findings reveal BMP signaling as essential regulator of zebrafish heart regeneration, and indicate that the difference in the capacity to regenerate the heart in fish and mammals could be related to differential responses of cardiomyocytes to activation of the same signaling pathway.

RESULTS

Tomo-Seq Reveals Distinct Molecular Regions within the Injured Heart

Zebrafish myocardial regeneration occurs via proliferation of differentiated cardiomyocytes, which in response to ventricular resection have been shown to dedifferentiate and re-enter the cell-cycle (Jopling et al., 2010; Kikuchi et al., 2010). The location of dedifferentiating cardiomyocytes, however, has not been well characterized following cryoinjury-induced necrotic lesions. At 7 days post cryoinjury (dpi), we observed that cardiomyocytes within about 50 μm of the wound border displayed reduced expression of the *myl7*:GFP transgene, a marker of differentiated cardiomyocytes (Figure 1A). Information on sample numbers for this and other experiments is shown in Table S1. These GFP^{low} cardiomyocytes also displayed other signs of dedifferentiation, namely disassembled sarcomeric structures (Figure S1A), reduced expression of the contractile protein Myomesin (Figure S1B), and activation of regulatory sequences of the *gata4* gene (Figure S1C) (Gupta et al., 2013; Szibor et al., 2014). In addition, GFP^{low} cardiomyocytes also upregulated markers of cell-cycle activity and mitosis (Figures 1A, 1B, and S1D).

To identify molecular signatures specific to this zone of dedifferentiating cardiomyocytes, we applied tomo-seq (Junker et al., 2014). For this purpose, cryoinjured hearts (at 3 and 7 dpi) were cryosectioned starting from the injury area into the healthy, uninjured myocardium (Figure 1C) and isolated RNA from each section was subjected to RNA sequencing (RNA-seq). Three to five million reads were sequenced, which mapped to ~15,000 genes (Data S1). To investigate global patterns of gene expression in our dataset, we performed Pearson's correlation analysis across all genes for each pairwise combination of sections. Interestingly, we observed several blocks of contiguous sections that are positively correlated to each other (3 dpi data presented in Figure 1D, 7 dpi data not shown), suggesting that the injured heart can be sub-divided into regions with specific molecular profiles based on gene expression patterns. To identify such regions, we performed hierarchical clustering of genes that show a clear expression peak (Z score > 1 in > 4 consecutive sections). The resulting plot confirmed that at least three distinct zones are present in the regenerating heart at 3 dpi: zone I (sections 1–6), zone II (sections 7–18), and zone III (sections 19–40) (Figure 1E). Next, we sought to verify these zones and analyze them in more detail. By calculating the log2-transformed fold change of the Z score for every gene between a zone of interest and the other

(E) Hierarchical clustering of Z score transformed expression profiles of all genes with expression peak (Z score > 1 in > 4 consecutive sections) in the 3 dpi heart. Zones I to III are marked by dashed yellow lines.

(F) Results of GO-term analysis using GOrilla for genes with spatially restricted expression in zones I, II, and III (based on gene lists in Data S2, S3, and S4) in the 3 dpi heart.

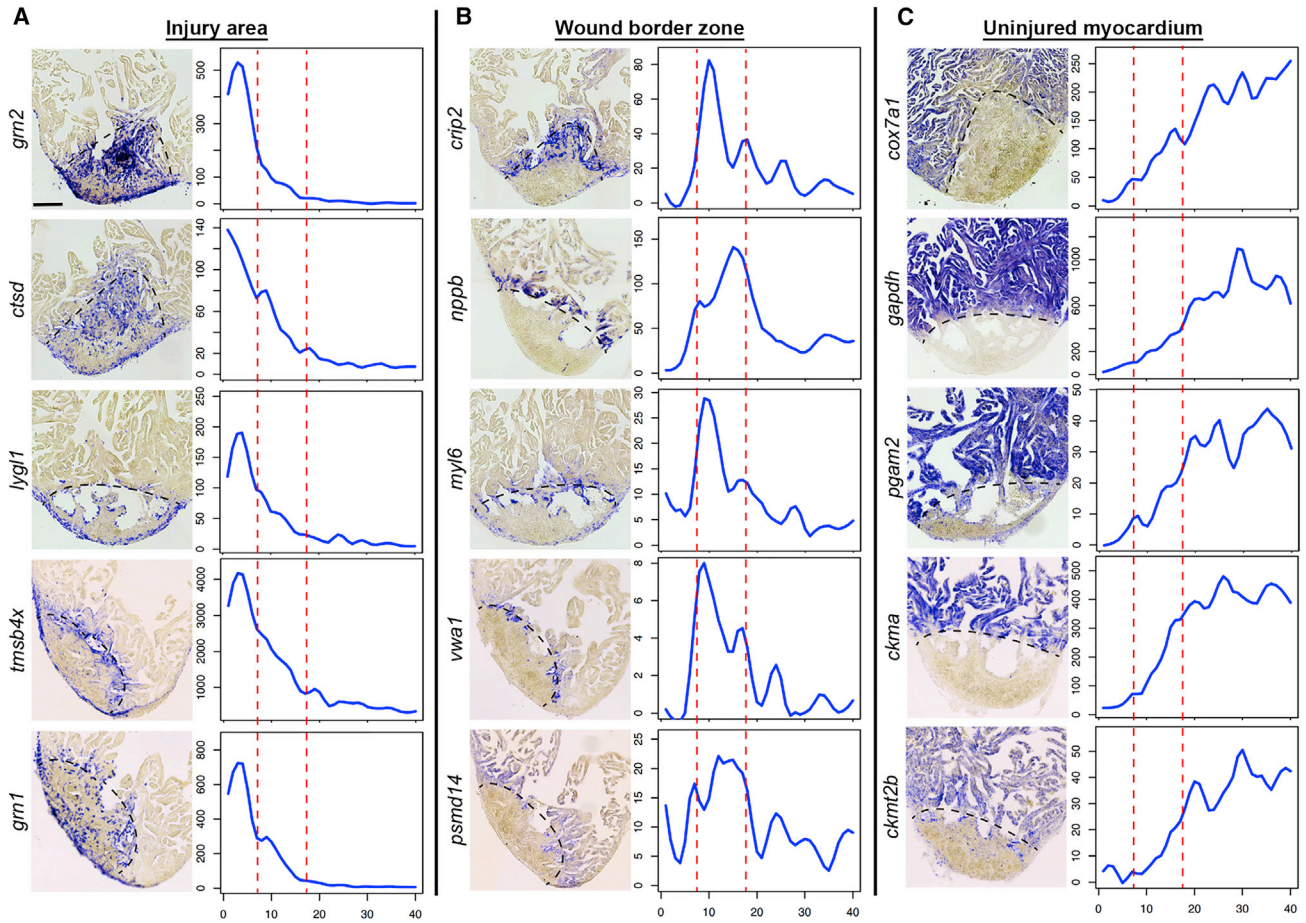

Figure 2. In Situ Hybridization Validates Tomo-Seq Results

In situ hybridization for genes identified by tomo-seq to be enriched in the injury area (zone I) (A), wound border zone (zone II) (B), or the uninjured myocardium (zone III) (C) at 3 dpi (n = 3). Left: representative in situ staining; right: expression traces from tomo-seq data. y axis, read counts; x axis, section number. Scale bar, 100 μm. Dashed black line indicates wound boundary on sections. Red lines in plots surround the border zone.

zones, ranked lists of spatially upregulated genes were generated (Data S2, S3, and S4). Analysis of the ranked lists of the different zones (by visual analysis of the gene expression traces) indicated that at 3 dpi more than 1,000 genes have enriched expression in one of the three zones (408 genes in zone I, 261 genes in zone II, and 362 genes in zone III). Interestingly, 10% of the genes with spatially enriched expression (114 genes) have not been functionally annotated in any system. Gene ontology (GO)-term analysis of the genes expressed in the different regions revealed that genes with an expression peak in zone I were associated with "translation," "embryo development," and "immune response." Interestingly, genes with expression peaks in zone II were most significantly linked to "regeneration," "protein folding," and "developmental growth," while genes with an expression peak in zone III were associated with "ATP metabolic process," "ventricular cardiac myofibril assembly," and "heart contraction" (Figure 1F). This indicates that zones I, II, and III correspond to the injury area, the wound border zone, where a regenerative program is activated, and the uninjured myocardium, respectively. To validate expression patterns identified by tomo-seq, we performed in situ hybridizations for top-ranked genes in each list on sections of cryoinjured hearts at 3 dpi. The eight selected genes upregulated in zone I indeed showed restricted expression in the wound including the epicardium overlaying it (Figure 2A and data not shown), confirming that zone I corresponds to the injury area. Among the tested genes are several wound healing response genes, e.g. *thymosinβ4* (*tmsb4x*), *granulin* (*grn1*, *grn2*), and *cathepsin D* (*ctsd*). For zone II the eight selected genes showed expression in between the injury area and the uninjured myocardium, confirming that zone II represents the wound border zone (BZ; Figure 2B and data not shown). Most prominent in the list of BZ genes is *natriuretic peptide B* (*nppb*), a cardiac hormone that is induced in response to myocardial stress in the mammalian heart and after ventricular resection in zebrafish (Gupta et al., 2013; Sergeeva et al., 2014). Of the eight tested genes upregulated in zone III, six showed a restricted expression in the uninjured myocardium by in situ hybridization (Figure 2C), while the remaining two genes (*acta1b* and *atp5b*) showed strong expression in the uninjured myocardium and weaker expression in the entire epicardium (data not shown). These results indicate that zone III represents the uninjured area. This is consistent with the observation

that many genes expressed in this region have a known role in muscle function (*ckmt2b*, *fabp3*, *cox7a1*, *acta1b*, *pgam2*, *casq2*, and *ckma*).

In summary, tomo-seq can identify the wound area, border zone, and uninjured myocardium in an unbiased manner simply based on spatially resolved genome-wide gene expression data. The resulting molecular profiles specific for these domains should facilitate identification of regulators of heart regeneration. The analyzed data for 3 and 7 dpi are available on our Web page http://zebrafish.genomes.nl/tomoseq/, providing a database that allows for easy searching of gene expression traces.

Spatially Restricted Gene Expression Reveals Two Distinct Border Zone Regions

Careful inspection of the hierarchical gene cluster analysis suggested the presence of sub-clusters in the border zone (region II in Figure 1E). Clustering of genes with a *Z* score of >1 in >3 consecutive sections identified two sub-clusters, one corresponding to genes expressed in the border zone further apically near the injury area (BZinj), and the other in the border zone further basally near the uninjured myocardium (BZmyo) (Figure 3A). Lists of genes upregulated in these two zones were generated in the same manner as described above (Data S5 and S6). In situ hybridization with the top-rated genes of both the BZinj and the BZmyo on consecutive sections of the same injured heart confirmed their expression in two spatially distinct regions (Figure S2A). Expression of the BZinj genes *crip2* and *ywhabl* overlapped with the endothelial marker *kdrl*, suggesting an endothelial character of BZinj cells. Furthermore, the BZinj showed upregulation of genes known for their expression in vascular endothelium (*vwa1*, *cldn5b*, and *mmrn2b*) and of smooth muscle cell markers (e.g. *myl6*, *junbb*, *crip2*, and *tagln*, encoding SM22a) (Figures 3B and S2B). Importantly, smooth muscle markers are known to be upregulated in myofibroblasts, which form in response to tissue injury and contribute to the wound repair process (reviewed in Hinz et al., 2007).

Interestingly, the BZmyo was enriched with genes that are highly expressed in the embryonic myocardium (e.g. *nppb*, *vmhc*, *actc1*, and *desma*), which regulate cardiac hypertrophy in mammals (e.g. *igf2b*) or control the cell cycle (e.g. *cyclinE* [*ccne2*], *brcc3*, *psmd14*, and *E2F1*) (Figures 2B, 3C, and S2B). Moreover, we observed that while *vmhc-like* (the ortholog of mammalian MYH7; Shih et al., 2015) is expressed throughout the myocardium, *vmhc* (the MYH6 ortholog) is upregulated in the BZmyo (Figure 3D). Immunofluorescence confirmed that Vmhc is expressed in embryonic, but not adult hearts, yet is upregulated specifically in dedifferentiating cardiomyocytes at the wound border in cryoinjured hearts (Figure 3E). These findings indicate that expression switching from adult to embryonic myosins occurs in the injured zebrafish heart, as it does in mammals.

Together these results suggest that two border zone regions with distinct gene expression profiles can be identified in the cryoinjured zebrafish heart. While the apical, injury-abutting border zone shows profiles characteristic of fibrosis and vasculogenesis, the myocardial border zone is characterized by the induction of embryonic myocardial genes, growth factors, and genes controlling the cell cycle.

BMP Signaling Is Specifically Activated in the Border Zone

Interestingly, several genes with known roles in BMP signaling or known BMP target genes were enriched in the two border zones (e.g. *acvr1l* [*alk8*], *smad1*, *id1*, *id2b*, *junbb*, *sall1b*, and *rgma*) (Figure 4A and data not shown). In situ hybridization confirmed the upregulation of the BMP target genes *id1* and *id2b*, the BMP ligands *bmp2b* and *bmp7*, and the type-I BMP receptor *bmpr1aa* (*alk3a*) in multiple cell types located in the border zone at 3 dpi (Figure 4B and data not shown). Expression of *bmp2b*, *bmp7*, and *bmpr1aa* continued to be enhanced at the wound border zone at 7 dpi, but was also upregulated in the epicardium covering the wound at this stage. Using accumulation of phosphorylated Smad1/5/8 in the nucleus as readout, we observed that BMP signaling was inactive in sham-operated adult zebrafish hearts but was activated in cardiomyocytes in the BZmyo from 1 dpi, where it increased by 3 dpi and persisted until at least 7 dpi (Figures 4C and 4D). In addition, BMP signaling activity was observed in both the endocardium and the epicardium at 3 dpi (Figure S3A). Taken together, these results suggest that BMP signaling activation is an injury response in the zebrafish heart, as it is in the injured mammalian heart. Interestingly however, pathway activation appears to occur later after injury and/or to persist longer than in mammalian hearts (Pachori et al., 2010).

Heart Regeneration Depends on BMP Signaling and Is Enhanced by BMP Overactivation

We next investigated whether BMP signaling is detrimental to or required for zebrafish heart regeneration. To block BMP signaling, we overexpressed the secreted BMP antagonist *noggin3* in heat-shock-inducible *hsp70l*:nog3 transgenic fish (Chocron et al., 2007), which was sufficient to drastically reduce nuclear pSmad1/5/8 expression in cardiomyocytes within 6 hr (Figure 5A). In zebrafish, cryoinjury-induced lesions of about 15–20% of the ventricle are regenerated within 60–120 days, and the wound shrinks to about one-fourth of its size within 21 days (Chablais et al., 2011; Schnabel et al., 2011). To assess whether BMP signaling is required for heart regeneration, we continuously inhibited BMP signaling via daily heat-shock of *hsp70l*:nog3; *myl7*:GFP double transgenic fish and quantified the *myl7*:GFP-negative wound area at 21 dpi. Interestingly, *noggin3*-expressing fish displayed significantly larger wounds than *myl7*:GFP single transgenic siblings that underwent the same heat-shock regime (Figure 5B). Assessment of wound size based on collagen and fibrin detection showed similar results in *hsp70l*:nog3 transgenics, which were heat-shocked daily from 3 to 21 dpi (Figure 5C). In addition, the healthy myocardial tissue expressing the *myl7*:GFP transgene was smaller in *noggin3*-expressing hearts (Figure S3B). We conclude that endogenous BMP signaling is required for zebrafish heart regeneration.

Next, we asked whether overactivation of BMP signaling can enhance heart regeneration. Heat-shock-induced overexpression of *bmp2b* in *hsp70l*:bmp2b transgenics (Chocron et al., 2007) was sufficient to induce accumulation of nuclear pSmad1/5/8 in uninjured hearts (Figure S3C) and to enhance the expression of the BMP target gene *id1* in injured hearts (Figure S3D). We continuously overexpressed *bmp2b* via daily heat shock starting at 1 dpi. At 7 dpi, no differences in wound size

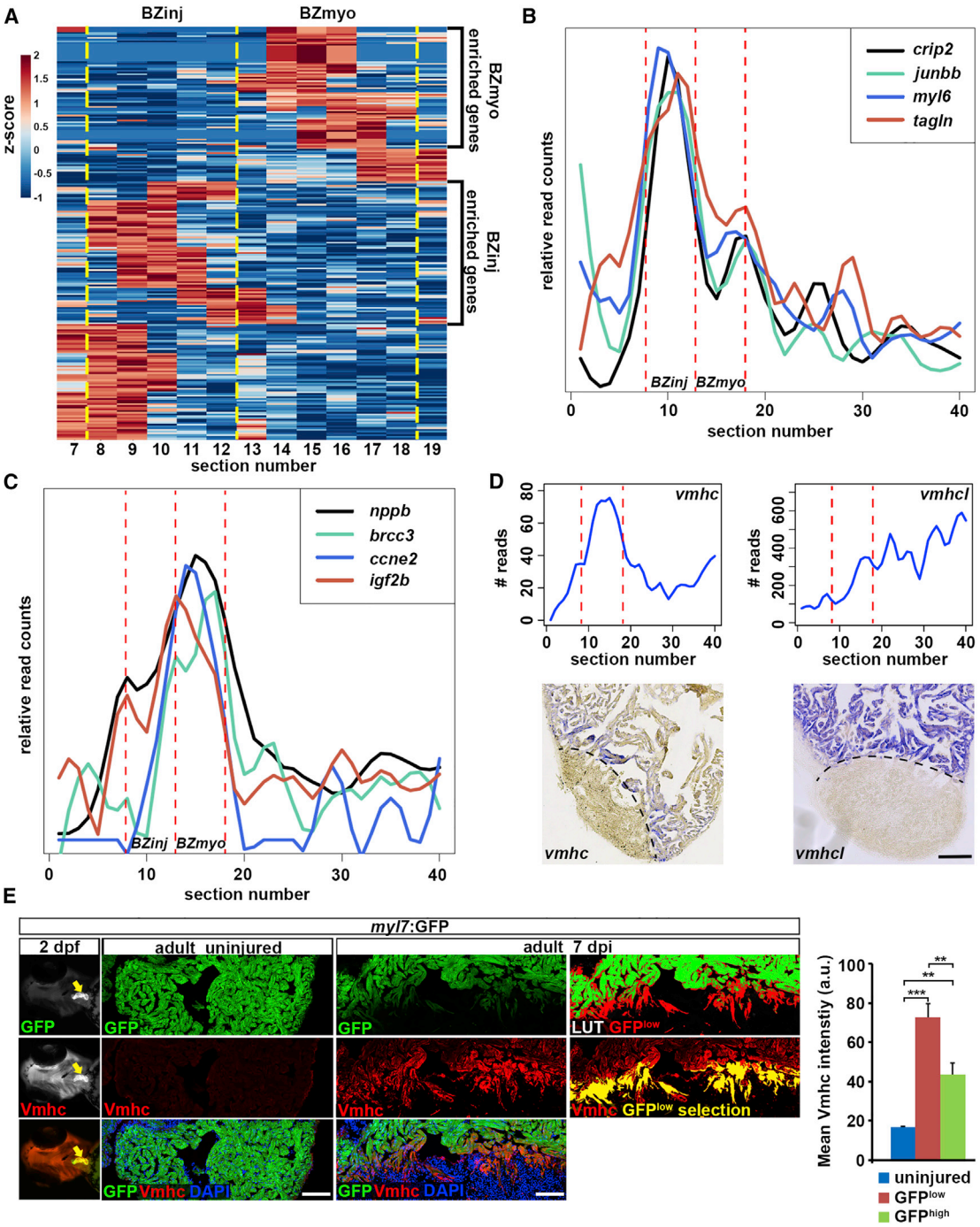

Figure 3. The Wound Border Zone Can Be Subdivided Based on Distinct Expression Profiles

(A) Cluster analysis on all genes with expression peaks in greater than three consecutive sections in the border zone (sections 8–18) of the 3 dpi heart identifies two sub-regions showing different expression patterns. Color spectrum indicates *Z* score. BZinj and BZmyo are marked by dashed yellow lines.

(B) Expression traces from tomo-seq data on cryoinjured heart (3 dpi) for selected genes showing peak expression in the BZinj region.

(C) Expression traces from tomo-seq data on cryoinjured heart (3 dpi) for selected genes showing peak expression in the BZmyo region.

(D) Expression traces from tomo-seq data and in situ hybridization on cryoinjured heart (3 dpi) for the myosin heavy chain (MHC) genes *vmhc* and *vmhc-like* (*vmhcl*). Scale bar, 100 μm.

(E) Ventricular myosin heavy chain (Vmhc) expression is detected in the developing heart of *myl7*:GFP transgenic embryos at 2 days post fertilization (arrow), but not in uninjured adult hearts. Vmhc is again expressed in GFP^{low} cardiomyocytes at 7 dpi. In LUT (lookup table) images, GFP intensity below 30% of signal intensity is displayed in red (GFP^{low}) while the rest is displayed in green (GFP^{high}). Note the overlapping expression pattern between GFP^{low} area (depicted as GFP^{low} selection) and Vmhc. Average Vmhc signal intensity in uninjured, GFP^{low}, and GFP^{high} cardiomyocytes at 7 dpi is plotted on the right. Error bars represent SEM. Student's t test, ***p = 0.0008 (uninjured versus GFP^{low}), **p = 0.002 (uninjured versus GFP^{high}), **p = 0.004 (GFP^{low} versus GFP^{high}). Scale bar, 50 μm.

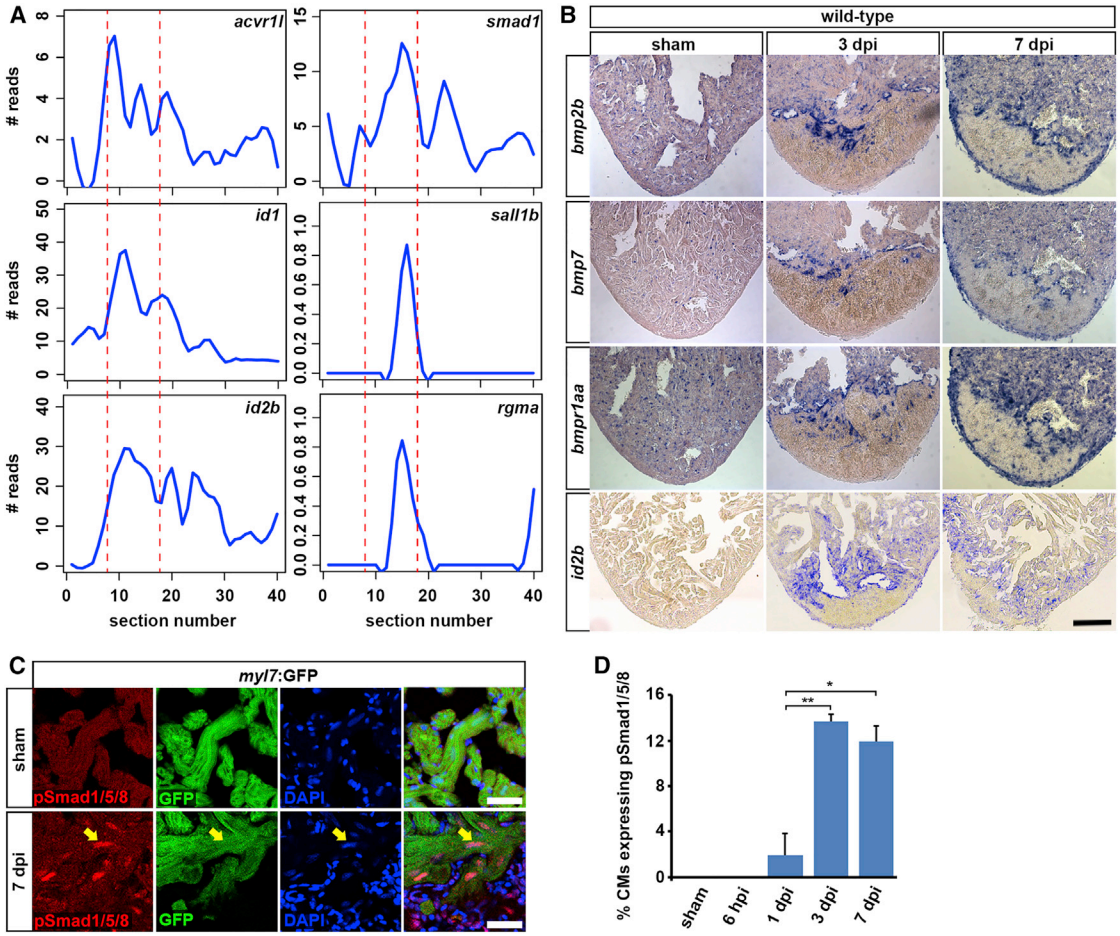

Figure 4. BMP Signaling Is Activated in Border Zone Cardiomyocytes

(A) Expression traces from tomo-seq data on cryoinjured heart (3 dpi) for BMP signaling-related genes reveal peak expression in the wound border zone (indicated by dashed lines).

(B) In situ hybridizations on sham-operated and 3 and 7 dpi hearts for the BMP ligands *bmp2b* and *bmp7*, the BMP receptor *bmpr1aa* (*alk3a*), and the BMP target gene *id2b*. Scale bar, 100 μm.

(C) At 7 dpi, nuclear pSmad1/5/8 expression (arrow) is detected in *myl7*:GFP-positive cardiomyocytes at the wound border. Scale bar, 25 μm.

(D) Average percentage of cardiomyocytes at the wound border expressing nuclear pSmad1/5/8 at different time points after cryoinjury. Error bars represent SEM. Student's t test, *p = 0.011, **p = 0.004.

between *hsp70l*:bmp2b; *myl7*:GFP double transgenics and heat-shocked *myl7*:GFP single transgenic siblings could be detected, confirming that the cryoinjury were of similar size in both groups (Figure S3E). In contrast, at 21 dpi the *myl7*:GFP-negative area in hearts overexpressing *bmp2b* was 60% of the size of that observed in siblings (Figure 5B), and collagen- and fibrin-containing wound tissue likewise was massively reduced (Figure 5C). In addition, *bmp2b* overexpression increased the size of healthy myocardial tissue (Figure S3B). Thus, prolonged overexpression of *bmp2b* is sufficient to enhance zebrafish heart regeneration.

BMP Signaling Promotes Cardiomyocyte Dedifferentiation

To understand how BMP signaling regulates heart regeneration, we assessed the cellular responses of different cardiac tissues to BMP inhibition. Reactivation of developmental gene programs in the endocardium and the epicardium has been identified as early response to heart injury (Gonzalez-Rosa et al., 2011; Kikuchi et al., 2011; Schnabel et al., 2011). However, treatment with the BMP type-I receptor antagonist dorsomorphin interfered neither with endocardial expression of *aldh1a2*, the rate-limiting enzyme in the synthesis of retinoic acid, which regulates cardiomyocyte proliferation (Kikuchi et al., 2011), nor with *wt1b*:GFP expression, a marker for the activated epicardium (Gonzalez-Rosa et al., 2011; Schnabel et al., 2011) (Figures S4A and S4B). These results suggest that BMP signaling is not required for activation of the regenerative response in the endocardial and epicardial layers.

We then concentrated on putative functions of BMP signaling in cardiomyocyte regeneration. Since BMP signaling has been implicated both positively (Ebelt et al., 2013) and negatively (Mungrue et al., 2011; Pachori et al., 2010) in mammalian cardiomyocyte survival following insults, we asked whether BMP pathway activity is required for cardiomyocyte survival in regenerating

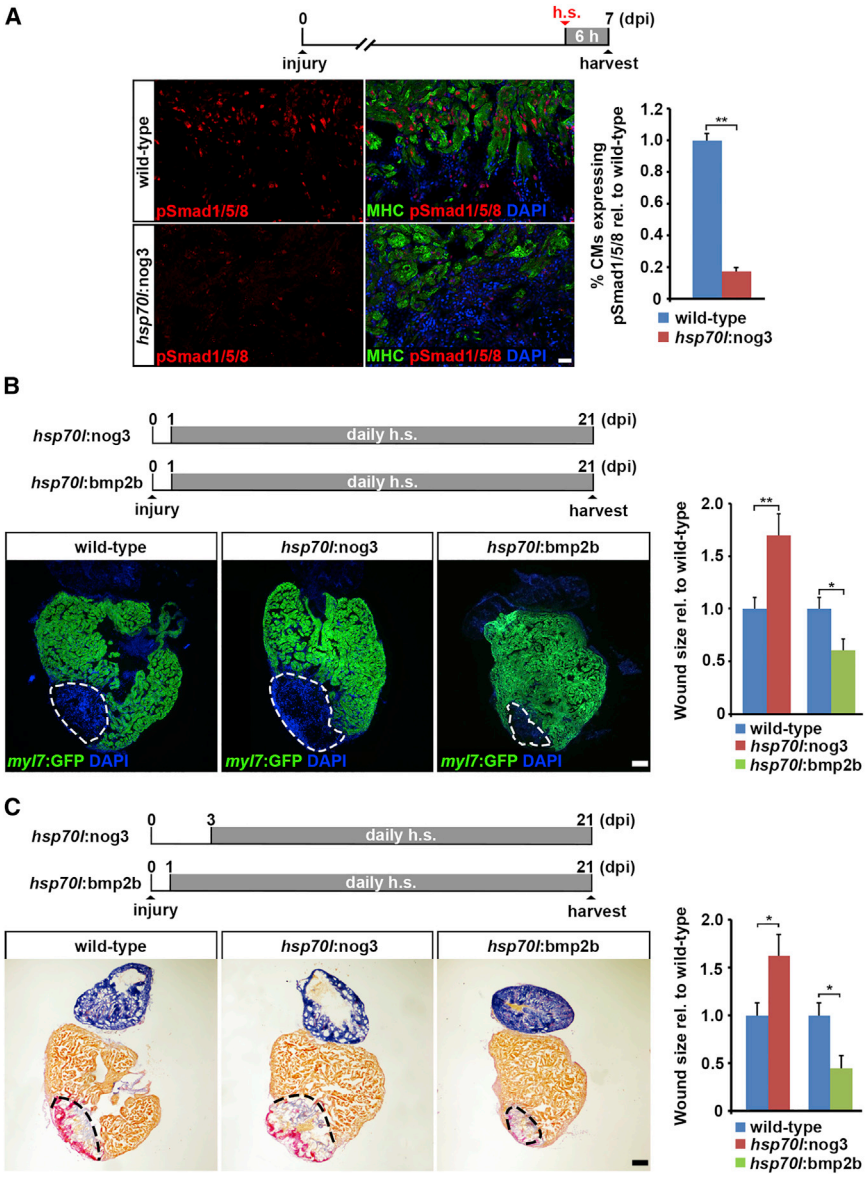

Figure 5. BMP Signaling Is Required for Myocardial Regeneration and Is Sufficient to Enhance It

(A) Expression of *noggin3* in *hsp70l*:nog3 transgenics for 6 hr is sufficient to significantly reduce nuclear pSmad1/5/8 accumulation in cardiomyocytes (CMs; positive for myosin heavy chain, MHC) at the wound border at 7 dpi. h.s., heat shock. Average percentage of cardiomyocytes expressing pSmad1/5/8 relative to that in wild-type hearts is plotted. Error bars represent SEM. Student's t test, **p = 0.003. Scale bar, 25 μm.

(B) GFP immunofluorescence analysis reveals wound size (dashed lines) at 21 dpi on heart sections of *hsp70l*:nog3; *myl7*:GFP, and *hsp70l*:bmp2b; *myl7*:GFP double transgenics and their respective *myl7*:GFP-only siblings (labelled "wild-type") subjected to the depicted heat-shock regime. Size of the GFP-negative area relative to the whole ventricle and normalized to heat-shocked *myl7*:GFP-only siblings is plotted. Error bars represent SEM. Student's t test, **p = 0.0081 (nog3), *p = 0.018 (bmp2b). Scale bar, 100 μm.

(C) Acid fuchsin orange G (AFOG) staining reveals wound size (dashed lines) at 21 dpi on heart sections of *hsp70l*:nog3, *hsp70l*:bmp2b transgenics and wild-type siblings subjected to the depicted heat-shock regime. Size of the wound tissue (red and purple staining) relative to the whole ventricle and normalized to heat-shocked wild-type siblings is plotted on the right. Error bars represent SEM. Student's t test, *p = 0.002 (nog3), *p = 0.016 (bmp2b). Scale bar, 100 μm.

zebrafish hearts. While we detected only few terminal deoxynucleotide transferase-mediated dUTP nick-end labeling (TUNEL)-positive apoptotic cardiomyocytes at the wound border at 1, 3, and 7 dpi (Figure 6A), *bmp2b* overexpression was sufficient to reduce their number even further (Figure 6B). In contrast, BMP inhibition by *noggin3* overexpression from 1 to 7 dpi did not enhance cardiomyocyte apoptosis (Figure 6B), arguing against an essential role of endogenous BMP signaling in protecting zebrafish cardiomyocytes from injury-induced cell death.

Since we found that BMP signaling is activated in cardiomyocytes of the BZmyo, we asked whether it is required for cardiomyocyte dedifferentiation, a cellular response to injury in this region, which has been suggested to contribute to heart regeneration (Jopling et al., 2010; Kikuchi et al., 2010; Wang et al., 2011). A significantly higher fraction of cardiomyocytes with low *myl7*:GFP expression (GFP^{low}) (25%) than with high *myl7*:GFP expression (GFP^{high}) (9%) was positive for nuclear pSmad1/5/8, indicating that BMP signaling activation is correlated with cardiomyocyte dedifferentiation (Figure 6C). We then investigated a potential function of BMP signaling in cardiomyocyte dedifferentiation by examining *myl7*:GFP downregulation and fetal myosin re-expression in the BZmyo. Both overexpression of *noggin3* and treatment with dorsomorphin from 3 to 7 dpi, which significantly suppressed nuclear pSmad1/5/8 accumulation in cardiomyocytes (Figure 6D), reduced the area of GFP^{low} cardiomyocytes in *myl7*:GFP transgenics at the wound border by half (Figure 6E). In contrast, wound size was not significantly altered by BMP signaling inhibition within this time frame (Figure S5A), showing that the reduced cardiomyocyte dedifferentiation was not a consequence of different extents of injury. Similarly, the re-expression of fetal myosin was also significantly reduced upon dorsomorphin treatment (Figure S5B). These results indicate that BMP signaling is required for dedifferentiation of cardiomyocytes at the wound border after injury.

BMP Signaling Is Required for Injury-Induced, but Not Physiological, Cardiomyocyte Proliferation

Cardiomyocyte dedifferentiation is a process that presumably occurs only early—within about 1 week—post injury. To test whether BMP signaling regulates heart regeneration primarily

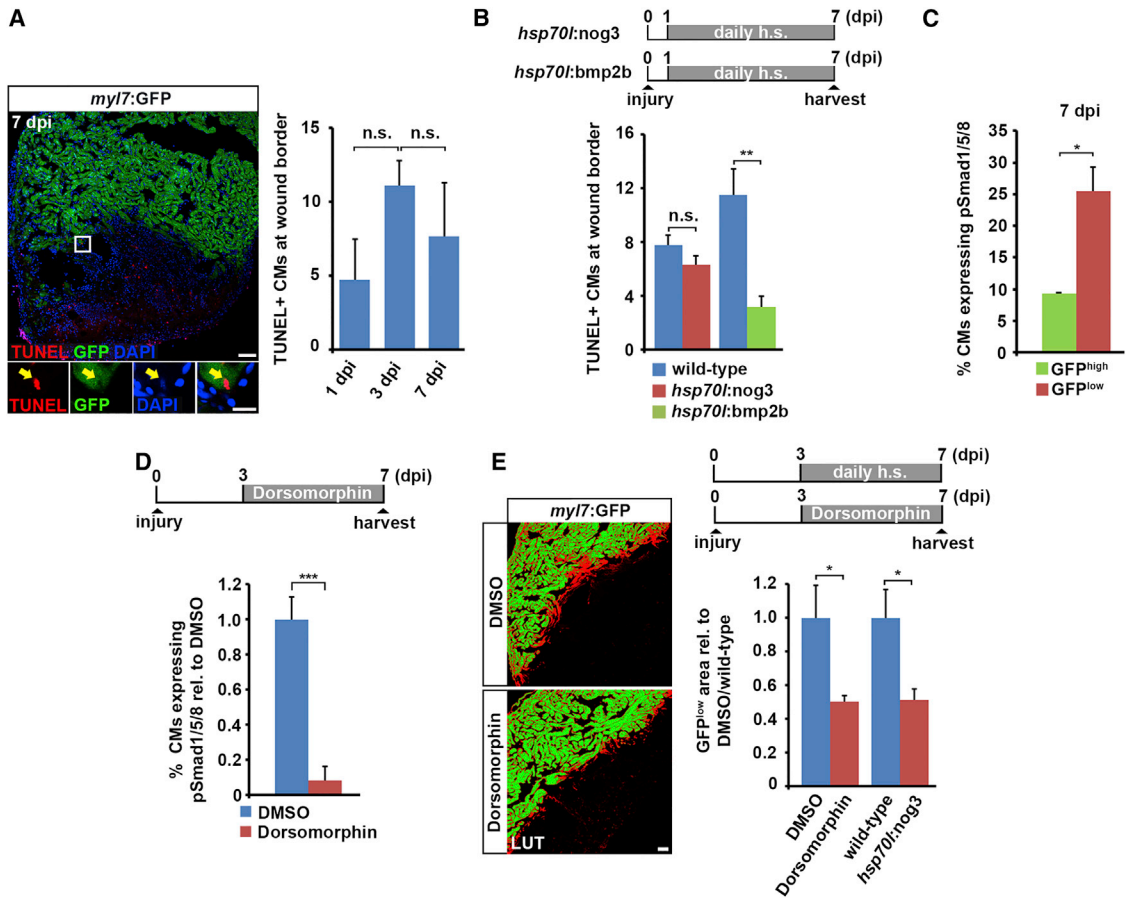

Figure 6. BMP Signaling Is Required for Cardiomyocyte Dedifferentiation but Not Survival

(A) TUNEL staining on sections of *myl7*:GFP hearts at 7 dpi. Magnified view (boxed area) shows an example of an apoptotic cardiomyocyte (yellow arrow). Average absolute number of TUNEL+ cardiomyocytes per section found at the wound border at different time points post injury is plotted. Error bars represent SEM. Student's t test, not significant (n.s.), p = 0.13 (1 versus 3 dpi), p = 0.45 (3 versus 7 dpi). Scale bars, 50 μm (overview), 12.5 μm (inset).

(B) The number of TUNEL+ cardiomyocytes at the wound border at 7 dpi does not significantly change in *hsp70l*:nog3 transgenics relative to heat-shocked wild-type siblings, while it is reduced in *hsp70l*:bmp2b transgenics. Error bars represent SEM. Student's t test, p = 0.38 (nog3) (not significant), **p = 0.004 (bmp2b). Scale bars, 50 μm (overview), 12.5 μm (inset).

(C) Average percentage of pSmad1/5/8 expressing GFP^{low} and GFP^{high} cardiomyocytes in *myl7*:GFP transgenic hearts at 7 dpi. Error bars represent SEM. Student's t test, *p = 0.014.

(D) Treatment of *myl7*:GFP transgenic fish with 5 μM dorsomorphin for 4 days significantly reduces nuclear pSmad1/5/8 accumulation in cardiomyocytes at the wound border at 7 dpi. Average percentage of cardiomyocytes expressing pSmad1/5/8 relative to DMSO control is plotted. Error bar represents SEM. Student's t test, ***p = 0.0002.

(E) Cardiomyocyte dedifferentiation, as monitored by the size of the GFP^{low} area in *myl7*:GFP transgenic hearts at 7 dpi, is reduced upon BMP signaling inhibition either by treatment with 5 μM dorsomorphin or by *noggin3* overexpression for 4 days. Error bars represent SEM. Student's t test, *p = 0.013 (dorsomorphin), *p = 0.025 (nog3). Scale bar, 50 μm.

because it is required for cardiomyocyte dedifferentiation, we inhibited or overactivated BMP signaling in *hsp70l*:nog3 and *hsp70l*:bmp2b transgenics from 1 to 7 dpi and allowed them to further regenerate without heat shocks till 21 dpi. We found that BMP signaling modulation within the first week after injury was not sufficient to significantly alter wound size at 21 dpi (Figure S5C), suggesting that BMP signaling activity beyond the first week after injury is required for heart regeneration. We thus looked for additional cellular processes regulated by BMP signaling. Proliferation of cardiomyocytes is key for zebrafish heart regeneration (reviewed in Kikuchi and Poss, 2012). Thus, we examined whether BMP signaling activation correlates with cell-cycle re-entry of cardiomyocytes. We looked for co-localization of proliferating cell nuclear antigen (PCNA) and the cardiomyocyte marker Mef2 with a transcriptional reporter for BMP signaling (*BRE*:GFP) (Laux et al., 2011), and found that the number of GFP-positive cardiomyocytes was 5-fold higher among PCNA-positive cardiomyocytes than in the entire cardiomyocyte population (35% compared with 7%) (Figure 7A). Furthermore, throughout the early phase of regeneration (1, 2, 3, 5, and 7 dpi), the percentage of *BRE*:GFP-positive cardiomyocytes was positively correlated with the percentage of proliferating cardiomyocytes (Pearson's correlation coefficient: 0.76) (Figure S6A). These results show that BMP pathway activity is correlated with cell-cycle activity in cardiomyocytes.

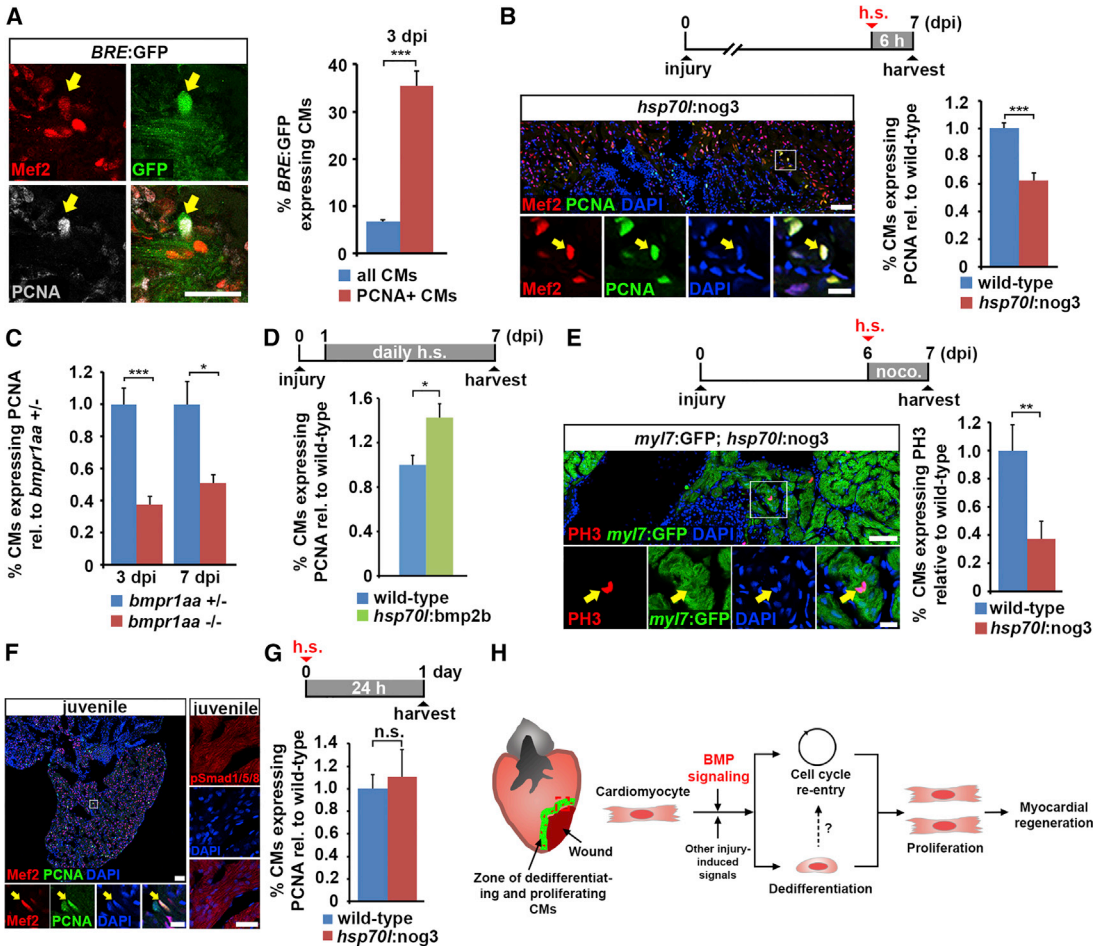

Figure 7. BMP Signaling is Required for Injury-Induced but Not Physiological Cardiomyocyte Proliferation

(A) Co-localization of Mef2 and PCNA with GFP (arrow), which reports BMP-mediated transcriptional activity in *BRE*:GFP transgenic hearts, at 3 dpi. Average percentages of PCNA+ and of all cardiomyocytes that express GFP are plotted. Error bars represent SEM. Student's t test, ***p = 0.000023.

(B) Expression of *noggin3* in *hsp70l*:nog3 transgenics for 6 hr is sufficient to reduce PCNA expression in cardiomyocytes (identified by nuclear Mef2, arrow) at the wound border at 7 dpi. Boxed area is shown as magnified view. Average percentage of cardiomyocytes expressing PCNA relative to wild-type is plotted. Error bars represent SEM. Student's t test, ***p = 0.00095. Scale bar, 50 μm.

(C) Hearts homozygous for a loss-of-function mutation of the BMP type-I receptor *bmpr1aa* display reduced expression of PCNA in cardiomyocytes (identified by nuclear Mef2) at the wound border at 3 and 7 dpi compared with *bmpr1aa*+/− hearts. Average percentage of cardiomyocytes expressing PCNA relative to *bmpr1aa*+/− control is plotted. Error bars represent SEM. Student's t test, ***p = 0.0002 (3 dpi), *p = 0.01 (7 dpi).

(D) Overexpression of *bmp2b* for 6 days via daily heat shock is sufficient to increase PCNA expression in cardiomyocytes at the wound border in *hsp70l*:bmp2b transgenics relative to heat-shocked wild-type siblings at 7 dpi. Average percentage of cardiomyocytes expressing PCNA relative to wild-type is plotted. Error bars represent SEM. Student's t test, *p = 0.011.

(E) Expression of *noggin3* for 24 hr in *hsp70l*:nog3; *myl7*:GFP double transgenics that were treated with 5 μM nocodazole reduces the percentage of phospho-Histone 3 (PH3)+ mitotic cardiomyocytes (arrow). Boxed area is shown as magnified view. Average percentage of cardiomyocytes expressing PH3 relative to wild-type is plotted. Error bars represent SEM. Student's t test, **p = 0.0068. Scale bar, 50 μm (overview) and 25 μm (magnified view).

(F) Many Mef2+ cardiomyocytes are also PCNA+ (arrow) in 9-week-old juvenile fish hearts, but no nuclear pSmad1/5/8 can be detected. Boxed area is shown as magnified view. Scale bar, 50 μm (overview and magnified view on the left) and 25 μm (pSmad1/5/8 staining on the right).

(G) Expression of *noggin3* in juvenile *hsp70l*:nog3 transgenics for 24 hr does not reduce the expression of PCNA in cardiomyocytes. Average percentage of cardiomyocytes expressing PCNA relative to wild-type is plotted. Error bars represent SEM. Student's t test, p = 0.67 (not significant).

(H) Model for BMP function during zebrafish heart regeneration. BMP signaling is activated in cardiomyocytes at the wound border and is required for cellular responses to injury in these cells, namely dedifferentiation and cell-cycle re-entry, and thus for cardiomyocyte proliferation and myocardial regeneration.

Next, we tested whether BMP signaling is required for cardiomyocyte cell-cycle re-entry. Short-term (6 hr) inhibition of BMP signaling by either *noggin3* overexpression or dorsomorphin treatment at 7 dpi significantly reduced PCNA expression in cardiomyocytes (Figures 7B and S6B). To validate these findings in a genetic model, we studied injury-induced cardiomyocyte proliferation in fish homozygous for a loss-of-function mutation in the BMP receptor *bmpr1aa* (Smith et al., 2011), which is expressed in the wound border zone in injured hearts (Figure 4B). While in double mutant embryos lacking both *bmpr1aa* and *bmpr1ab* cardiomyocyte specification is entirely lost, mutant embryos lacking only *bmpr1aa* display only mild larval defects

in organ laterality and dorsoventral patterning, and survive to adulthood without any discernible cardiac defects. In contrast, *bmpr1aa* function is required for heart regeneration, since *bmpr1aa* mutants showed fewer PCNA-positive cardiomyocytes than heterozygous control fish at 3 and 7 dpi (Figure 7C). On the other hand, overexpression of *bmp2b* from 1 to 7 dpi in *hsp70l*:bmp2b transgenics significantly enhanced PCNA expression in cardiomyocytes, particularly within 50 μm from the wound border (Figures 7D and S6C). Finally, we asked whether BMP signaling is also required for cardiomyocyte mitosis. Since the number of cardiomyocytes expressing phosphorylated histone H3 (PH3) at any particular time point during heart regeneration is very low (Sallin et al., 2015), which makes it difficult to attain statistically sound data on modulators of mitosis, we inhibited cytokinesis using nocodazole treatment and thus arrested cardiomyocytes in a PH3-positive state. Short-term inhibition (24 hr) of BMP signaling by *noggin3* overexpression (together with nocodazole treatment) strongly reduced the mitotic index of cardiomyocytes at 7 dpi (Figure 7E). Treatment with dorsomorphin for 1 or 4 days suppressed cardiomyocyte mitosis at 7 dpi as well (Figure S6D). Altogether, these data strongly indicate that BMP signaling promotes proliferation of spared cardiomyocytes following injury.

This finding prompted us to examine whether BMP signaling activity is also required for cardiomyocyte proliferation during physiological heart growth in juvenile zebrafish (Wills et al., 2008). While many cardiomyocytes were PCNA-positive in the juvenile heart at 8–9 weeks of age, we could not detect any nuclear pSmad1/5/8 expression in these hearts (Figure 7F). In addition, neither *noggin3* overexpression nor dorsomorphin treatment reduced the percentage of PCNA-positive cardiomyocytes in juvenile hearts (Figures 7G and S6E). Furthermore, while overexpression of *bmp2b* in *hsp70l*:bmp2b transgenics was sufficient to activate BMP signaling in uninjured adult hearts (Figure S3C), it did not induce cardiomyocyte proliferation in the absence of injury (Figure S6F). Together with the observation that *bmpr1aa* mutant hearts have normal morphology and size, these data reveal that BMP signaling specifically regulates injury-induced cardiomyocyte proliferation.

DISCUSSION

Here we applied tomo-seq, a technique we have recently established to obtain genome-wide RNA-seq data from embryos or tissues with spatial resolution, to the regenerating zebrafish heart. We were able to distinguish distinct regions in the regenerating heart solely based on their expression profiles. Most importantly, we identified two wound border zones with distinct expression profiles where processes essential for heart regeneration, namely cardiomyocyte dedifferentiation and proliferation, occur. This led to the discovery that BMP signaling is specifically activated in the border region. Our results suggest the following model for BMP signaling function during heart regeneration (Figure 7H). Physiological cardiomyocyte proliferation during heart growth in juvenile fish does not require BMP signaling. However, in injured hearts BMP signaling is activated in resident cardiomyocytes at the wound border. This pathway is essential for myocardial regeneration via regulating cardiomyocyte dedifferentiation and cell-cycle re-entry, cellular processes that are specifically activated after injury and do not occur in growing hearts. Experimental activation of BMP signaling in uninjured hearts, however, is not sufficient to induce cardiomyocyte cell-cycle re-entry, indicating that it acts with other injury-induced signals (Figure 7H). Thus, BMP signaling is an essential and injury-specific regulator of cardiomyocyte regeneration in the naturally regenerating zebrafish heart.

We show that the tomo-seq technique, which has thus far only been applied to embryos, works well to identify regions with specific expression profiles in isolated adult tissues. Several previous studies have used RNA-seq or microarray technology to identify expression profiles of entire regenerating zebrafish hearts (Lien et al., 2006; Sleep et al., 2010), and one study has used translational profiling to identify injury responses specifically in cardiomyocytes (Fang et al., 2013). Although these techniques are useful for differential gene expression analysis within a rather homogeneous tissue, they are of limited use for identifying genes specifically regulated in a small region of the tissue. Furthermore, conventional methods for obtaining spatial information of gene expression, such as in situ hybridization or immunohistochemistry, can only be applied to a limited set of candidates. We believe that the tomo-seq data generated for the regenerating heart will be useful for future studies into the mechanisms driving heart regeneration. In addition, our data show that there are many uncharacterized genes with spatially restricted expression in the injured heart that might have important functions.

While most signaling pathways that have been implicated in zebrafish heart regeneration are mainly active in the endocardium and/or epicardium (reviewed in Gemberling et al., 2013), BMP signaling is activated in proliferating cardiomyocytes after injury. Thus, together with Jak1/Stat3 signaling (Fang et al., 2013), BMP signaling is a good candidate for a pathway that directly affects cardiomyocyte regeneration. However, the cellular sources of BMP ligands remain to be identified. Our tomo-seq data and in situ hybridization analyses showed that expression of BMP ligands (*bmp2b* and *bmp7*) and the type-I BMP receptor (*bmpr1aa*) localizes to the border zone and appears to include both endocardial cells and cardiomyocytes. Further studies will be required to determine which BMP ligands are responsible for Smad1/5/8 signaling activation in cardiomyocytes and whether they act in a paracrine and/or autocrine fashion.

In zebrafish, cardiomyocytes modulate their differentiation state in response to heart injury, which includes upregulation of the regulatory sequence of *gata4* (our data and Kikuchi et al., 2010) and other cardiac transcription factors such as *tbx20* and *nkx2.5* (Lepilina et al., 2006). Since expression of these transcription factors is regulated by BMP signaling during heart development (de Pater et al., 2012; Liu et al., 2014; Mandel et al., 2010), it is possible that the pathway promotes cardiomyocyte dedifferentiation via regulation of these factors. Moreover, activated BMP signaling leads to the induction of *id* gene expression, encoding negative regulators of basic helix-loop-helix (bHLH) transcription factors (Ling et al., 2014). Expression of Id proteins is typically high in stem cells and progenitor cells, suggesting that they play a role in maintenance of the undifferentiated state (Liu et al., 2013; Ying et al., 2003). In addition, Id proteins can promote cell proliferation by regulating the expression

of cell-cycle genes (Prabhu et al., 1997). Our tomo-seq and in situ hybridization data demonstrate the upregulation of *id1* and *id2b* in the border zone, suggesting that BMP-mediated upregulation of Id proteins could play a role in the dedifferentiation and proliferation of cardiomyocytes possibly via the inhibition of bHLH transcription factors.

In cultured mammalian cardiomyocytes, exogenous BMP2 protein is able to induce cell-cycle activity (Chakraborty et al., 2013) while BMP4 protein has been shown to enhance apoptosis and hypertrophy (Sun et al., 2013). To clarify the role of BMP signaling in mammalian cardiomyocytes, we also compared the effects of BMP2 and BMP4 on neonatal rat cardiomyocyte in vitro. Addition of either protein did not induce cardiomyocyte proliferation, but caused hypertrophic responses including expression of *Nppa* (ANP) and increases in cell size (Figures S7A and S7B). Thus, we could not confirm the previously reported pro-proliferative role of BMP2 or a differential effect of BMP2 and BMP4 on cultured neonatal mammalian cardiomyocytes. However, such discrepancies could be attributed to different experimental setups, e.g. different ways of measuring cardiomyocyte proliferation (Ki67 versus BrdU incorporation).

While in vivo Noggin injection in mice reduces apoptosis and infarct size and improves functional recovery after MI, transgenic overexpression of *noggin3* in the zebrafish heart has no effect on cardiomyocyte apoptosis but significantly compromises cardiomyocyte regeneration (Pachori et al., 2010). These findings indicate that endogenous BMP signaling is activated by cardiac injury in both mammals and zebrafish but has opposite effects on cardiac repair. Whether these different outcomes can be attributed to different spatial and temporal activation profiles of BMP signaling, or to different downstream effectors and transcriptional targets in cardiomyocytes, remains to be elucidated. Nonetheless, our results indicate that in the search for molecular reasons for the differential ability of fish and mammals to regenerate the heart, it could be equally important to look for differentially regulated pathways and to identify how the heart reacts to signals that are regulated in response to injury in both fish and mammals.

In summary, we show that the spatial gene expression information provided by tomo-seq allows for the identification of molecular signals that regulate essential regenerative processes in the zebrafish heart. We anticipate that our detailed characterization of the border zone in the regenerating heart and the identification of BMP signaling as an important regulator of cardiomyocyte proliferation will help to find strategies in the future for stimulating the regenerative capacities of the mammalian heart.

EXPERIMENTAL PROCEDURES

Transgenic Fish Lines, Cryoinjury, Heat Shocks, and Dorsomorphin Treatment

All procedures involving animals were approved by the local animal experiments committees and performed in compliance with animal welfare laws, guidelines, and policies, according to national and European law.

Zebrafish of ~4–18 months of age were used, except for experiments with juvenile fish which were 8–9 weeks old. The following fish lines were used: *hsp70l*:nog3^{fr14Tg} (Chocron et al., 2007), *hsp70l*:bmp2b^{fr13tg} (Chocron et al., 2007), *wt1b*:GFP^{li3Tg} (Perner et al., 2007), *BRE*:GFP^{pt510Tg} (Laux et al., 2011), *myl7*:GFP^{twu34Tg} (Huang et al., 2003), *fli1a*:eGFP^{y1Tg} (Lawson and Weinstein, 2002), *-14.8gata4*:GFP^{ae1} (Heicklen-Klein and Evans, 2004), *bmpr1aa*^{hu4087} (Smith et al., 2011), Et(*krt4*:EGFP)^{sqet27} (Parinov et al., 2004), and *myl7*:dsRed2-NLS^{f2Tg} (Mably et al., 2003). Cryoinjuries were performed as previously described (Schnabel et al., 2011), except that a liquid nitrogen-cooled copper filament of 0.3-mm diameter was used instead of dry ice. For experiments involving heat-shock-inducible gene expression, fish were heat-shocked at 37°C for 1 hr, after which the water temperature was reduced back to 27°C within 15 min. For short-term experiments hearts were harvested 5 hr after the end of the heat shock, and for long-term experiments fish were heat-shocked once daily.

For drug treatment, dorsomorphin (Sigma P5499) or nocodazole (Sigma M1404) were applied at 5 μM in fish system water while DMSO was used as a solvent control.

Histological Methods, Immunofluorescence, and TUNEL Assay

For immunofluorescence and histological staining, hearts were extracted, fixed in 4% paraformaldehyde (PFA) (in phosphate buffer with 4% sucrose) at room temperature for 1 hr and cryosectioned into 10-μm sections. Heart sections were equally distributed onto seven serial slides so that each slide contained sections representing all areas of the ventricle.

Acid fuchsin orange G (AFOG) staining was performed on cryosections as previously described (Poss et al., 2002). Measurements of the size of ventricular areas (the wound area based on AFOG staining, the GFP^{low} cardiomyocyte area, and the area of fetal myosin expression) were performed manually with ImageJ (NIH) software on 2–4 sections containing the biggest wound (Schneider et al., 2012). Measurements of the size of the wound area and of the regenerated myocardium on sections of *myl7*:GFP hearts or on myosin heavy chain-immunostained sections on wild-type or transgenic hearts were performed manually with ImageJ software on all sections of one serial slide, representing approximately one-seventh of the total ventricle.

Primary antibodies used were anti-PCNA (Dako #M0879), anti-GFP (Abcam #ab13970), anti-PH3 (Cell-Signaling #9706), anti-pSmad1/5/8 (Cell-Signaling #9511), anti-Vmhc (Sigma #SAB2701875), anti-Aldhla2 (Abmart #P30011), anti-α-actinin (Sigma #A7811), anti-MF20 (Developmental Studies Hybridoma Bank), anti-Myomesin B4 (Developmental Studies Hybridoma Bank), and anti-Mef2c (Santa Cruz #SC313). For PCNA and Mef2c, antigen retrieval was performed by heating slides containing heart sections at 85°C in 10 mM sodium citrate buffer (pH 6) for 10 min. Secondary antibodies conjugated to Alexa 488, 555, or 633 (Invitrogen) were used at a dilution of 1:1,000. Nuclei were shown by DAPI (4′,6-diamidino-2-phenylindole) staining. All images of immunofluorescence stainings are single optical planes acquired with Leica Sp5 or Sp8 confocal microscopes. For quantifications, two to three sections displaying the biggest wounds were analyzed per heart. Quantifications of PCNA, Mef2, PH3, and TUNEL expression were performed in cardiomyocytes situated within 150 μm from the wound border unless otherwise specified.

For cardiomyocyte mitotic index estimation, the number of PH3-positive cardiomyocytes situated within 150 μm from the wound border in all sections from each heart containing an obvious wound area was counted. In those sections, the total number of cardiomyocytes was estimated by determining the average density of cardiomyocytes per μm^2 in three separate areas (size: 70 μm^2), and by multiplying this number by the total area size.

TUNEL staining was performed using ApoTag Red in situ kit (Millipore) on heart cryosections as per the manufacturer's instructions.

In Situ Hybridization

After overnight fixation in 4% PFA, hearts were washed in PBS twice, dehydrated in EtOH, and embedded in paraffin. Serial sections were made at 10 μm. In situ hybridization was performed on paraffin sections as previously described (Moorman et al., 2001), except that the hybridization buffer used did not contain heparin and yeast total RNA.

Tomo-Seq and Data Analysis

Cryoinjured zebrafish hearts were extracted at 3 or 7 dpi, and directly embedded in Jung tissue freezing medium (Leica). Hearts were cryosectioned starting from the injury area into the uninjured myocardium at 12-μm thickness and collected in separate tubes. RNA was extracted using Trizol (Ambion) after adding a defined amount of spike-in RNA to correct for technical variations

during the downstream processing. RNA-seq was performed as previously described (Junker et al., 2014) and is described in detail in Supplemental Experimental Procedures.

For correlation analysis, all genes expressed at >4 reads in >1 section were selected prior to total-read-normalization. Based on the log2-transformed-fold-change (zlfc) of the *Z* score (number of standard deviations above the mean) of all genes, the Pearson correlation was calculated across all genes for each pairwise combination of sections. Hierarchical cluster analysis on the entire dataset (after *Z* score transformation) was performed on all genes with a peak in >4 consecutive sections (*Z* score > 1). All genes with a peak in >3 consecutive sections were used for cluster analysis of the border zone (sections 8–18). Ranked lists of spatially upregulated genes were generated by calculating the zlfc for every gene between a zone of interest and the remaining zones. GO-term analysis on ranked lists was performed using the online tool GOrilla by submitting whole lists for GO-term analysis (Eden et al., 2009). Bioinformatic analyses were largely performed with R software using custom-written code (R Core Team, 2013). The correlation analysis and plot were generated in MATLAB (MathWorks).

ACCESSION NUMBERS

RNA-seq data are deposited on Gene Expression Omnibus, accession number GEO: GSE74652. The analyzed dataset is available on our Web page: http://zebrafish.genomes.nl/tomoseq/Kruse2015/.

SUPPLEMENTAL INFORMATION

Supplemental Information includes Supplemental Experimental Procedures, seven figures, one table, and six supplemental data files and can be found with this article online at http://dx.doi.org/10.1016/j.devcel.2015.12.010.

AUTHOR CONTRIBUTIONS

F.K. performed the tomo-seq, in situ hybridizations, and experiments on the *alk3* mutant and *BRE*:GFP fish. J.P.J., D.G., and A.v.O. assisted with the bioinformatics analysis. E.B. created the searchable database. D.C.Z. performed the experiments on cultured mammalian cardiomyocytes. M.D.V. performed the experiments on cardiomyocyte apoptosis. All other experiments were performed by C.-C.W. All authors designed the experiments and analyzed the data. C.-C.W., F.K., J.B., and G.W. wrote the paper.

ACKNOWLEDGMENTS

J.B. acknowledges support from the Netherlands Cardiovascular Research Initiative, the Dutch Heart Foundation, Dutch Federation of University Medical Centers, the Netherlands Organisation for Health Research and Development, and the Royal Netherlands Academy of Sciences. G.W. thanks Doris Weber and Brigitte Korte for fish care and technical help. This work was supported by a CVON grant (CVON2011-12 HUSTCARE) to J.B., a "Klaus-Georg und Sigrid Hengstberger-Forschungsstipendium" by the German Cardiac Society to G.W., a Deutsche Forschungsgemeinschaft grant ("Danger Response, Disturbance Factors and Regenerative Potential after Acute Trauma," CRC 1149) to G.W., and a EuFishBioMed Short-Term Fellowship to C.-C.W. This work was supported by an Emerging Fields Initiative for Cell Cycle in Disease and Regeneration from the Friedrich-Alexander-Universität Erlangen-Nürnberg (F.B.E.).

Received: April 17, 2015
Revised: October 14, 2015
Accepted: November 20, 2015
Published: December 31, 2015

REFERENCES

Bergmann, O., Bhardwaj, R.D., Bernard, S., Zdunek, S., Barnabe-Heider, F., Walsh, S., Zupicich, J., Alkass, K., Buchholz, B.A., Druid, H., et al. (2009). Evidence for cardiomyocyte renewal in humans. Science *324*, 98–102.

Chablais, F., Veit, J., Rainer, G., and Jazwinska, A. (2011). The zebrafish heart regenerates after cryoinjury-induced myocardial infarction. BMC Dev. Biol. *11*, 21.

Chakraborty, S., Sengupta, A., and Yutzey, K.E. (2013). Tbx20 promotes cardiomyocyte proliferation and persistence of fetal characteristics in adult mouse hearts. J. Mol. Cell Cardiol. *62*, 203–213.

Chocron, S., Verhoeven, M.C., Rentzsch, F., Hammerschmidt, M., and Bakkers, J. (2007). Zebrafish Bmp4 regulates left-right asymmetry at two distinct developmental time points. Dev. Biol. *305*, 577–588.

de Pater, E., Ciampricotti, M., Priller, F., Veerkamp, J., Strate, I., Smith, K., Lagendijk, A.K., Schilling, T.F., Herzog, W., Abdelilah-Seyfried, S., et al. (2012). BMP signaling exerts opposite effects on cardiac differentiation. Circ. Res. *110*, 578–587.

Ebelt, H., Hillebrand, I., Arlt, S., Zhang, Y., Kostin, S., Neuhaus, H., Muller-Werdan, U., Schwarz, E., Werdan, K., and Braun, T. (2013). Treatment with bone morphogenetic protein 2 limits infarct size after myocardial infarction in mice. Shock *39*, 353–360.

Eden, E., Navon, R., Steinfeld, I., Lipson, D., and Yakhini, Z. (2009). GOrilla: a tool for discovery and visualization of enriched GO terms in ranked gene lists. BMC Bioinformatics *10*, 48.

Fang, Y., Gupta, V., Karra, R., Holdway, J.E., Kikuchi, K., and Poss, K.D. (2013). Translational profiling of cardiomyocytes identifies an early Jak1/Stat3 injury response required for zebrafish heart regeneration. Proc. Natl. Acad. Sci. USA *110*, 13416–13421.

Gemberling, M., Bailey, T.J., Hyde, D.R., and Poss, K.D. (2013). The zebrafish as a model for complex tissue regeneration. Trends Genet. *29*, 611–620.

Gemberling, M., Karra, R., Dickson, A.L., and Poss, K.D. (2015). Nrg1 is an injury-induced cardiomyocyte mitogen for the endogenous heart regeneration program in zebrafish. Elife *4*, e05871.

Gonzalez-Rosa, J.M., Martin, V., Peralta, M., Torres, M., and Mercader, N. (2011). Extensive scar formation and regression during heart regeneration after cryoinjury in zebrafish. Development *138*, 1663–1674.

Gupta, V., Gemberling, M., Karra, R., Rosenfeld, G.E., Evans, T., and Poss, K.D. (2013). An injury-responsive gata4 program shapes the zebrafish cardiac ventricle. Curr. Biol. *23*, 1221–1227.

Heicklen-Klein, A., and Evans, T. (2004). T-box binding sites are required for activity of a cardiac GATA-4 enhancer. Dev. Biol. *267*, 490–504.

Hinz, B., Phan, S.H., Thannickal, V.J., Galli, A., Bochaton-Piallat, M.L., and Gabbiani, G. (2007). The myofibroblast: one function, multiple origins. Am. J. Pathol. *170*, 1807–1816.

Huang, C.J., Tu, C.T., Hsiao, C.D., Hsieh, F.J., and Tsai, H.J. (2003). Germ-line transmission of a myocardium-specific GFP transgene reveals critical regulatory elements in the cardiac myosin light chain 2 promoter of zebrafish. Dev. Dyn. *228*, 30–40.

Izumi, M., Fujio, Y., Kunisada, K., Negoro, S., Tone, E., Funamoto, M., Osugi, T., Oshima, Y., Nakaoka, Y., Kishimoto, T., et al. (2001). Bone morphogenetic protein-2 inhibits serum deprivation-induced apoptosis of neonatal cardiac myocytes through activation of the Smad1 pathway. J. Biol. Chem. *276*, 31133–31141.

Jopling, C., Sleep, E., Raya, M., Marti, M., Raya, A., and Izpisua Belmonte, J.C. (2010). Zebrafish heart regeneration occurs by cardiomyocyte dedifferentiation and proliferation. Nature *464*, 606–609.

Junker, J.P., Noel, E.S., Guryev, V., Peterson, K.A., Shah, G., Huisken, J., McMahon, A.P., Berezikov, E., Bakkers, J., and van Oudenaarden, A. (2014). Genome-wide RNA tomography in the zebrafish embryo. Cell *159*, 662–675.

Kikuchi, K., and Poss, K.D. (2012). Cardiac regenerative capacity and mechanisms. Annu. Rev. Cell Dev. Biol *28*, 719–741.

Kikuchi, K., Holdway, J.E., Werdich, A.A., Anderson, R.M., Fang, Y., Egnaczyk, G.F., Evans, T., Macrae, C.A., Stainier, D.Y., and Poss, K.D. (2010). Primary contribution to zebrafish heart regeneration by gata4(+) cardiomyocytes. Nature *464*, 601–605.

Kikuchi, K., Holdway, J.E., Major, R.J., Blum, N., Dahn, R.D., Begemann, G., and Poss, K.D. (2011). Retinoic acid production by endocardium and

epicardium is an injury response essential for zebrafish heart regeneration. Dev. Cell *20*, 397–404.

Laux, D.W., Febbo, J.A., and Roman, B.L. (2011). Dynamic analysis of BMP-responsive smad activity in live zebrafish embryos. Dev. Dyn. *240*, 682–694.

Lawson, N.D., and Weinstein, B.M. (2002). In vivo imaging of embryonic vascular development using transgenic zebrafish. Dev. Biol. *248*, 307–318.

Lepilina, A., Coon, A.N., Kikuchi, K., Holdway, J.E., Roberts, R.W., Burns, C.G., and Poss, K.D. (2006). A dynamic epicardial injury response supports progenitor cell activity during zebrafish heart regeneration. Cell *127*, 607–619.

Lien, C.L., Schebesta, M., Makino, S., Weber, G.J., and Keating, M.T. (2006). Gene expression analysis of zebrafish heart regeneration. PLoS Biol. *4*, e260.

Ling, F., Kang, B., and Sun, X.H. (2014). Id proteins: small molecules, mighty regulators. Curr. Top. Dev. Biol. *110*, 189–216.

Liu, H., Jia, D., Li, A., Chau, J., He, D., Ruan, X., Liu, F., Li, J., He, L., and Li, B. (2013). p53 regulates neural stem cell proliferation and differentiation via BMP-Smad1 signaling and Id1. Stem Cell Dev. *22*, 913–927.

Liu, Y., Harmelink, C., Peng, Y., Chen, Y., Wang, Q., and Jiao, K. (2014). CHD7 interacts with BMP R-SMADs to epigenetically regulate cardiogenesis in mice. Hum. Mol. Genet. *23*, 2145–2156.

Lu, J., Sun, B., Huo, R., Wang, Y.C., Yang, D., Xing, Y., Xiao, X.L., Xie, X., and Dong, D.L. (2014). Bone morphogenetic protein-2 antagonizes bone morphogenetic protein-4 induced cardiomyocyte hypertrophy and apoptosis. J. Cell Physiol. *229*, 1503–1510.

Mably, J.D., Mohideen, M.A., Burns, C.G., Chen, J.N., and Fishman, M.C. (2003). Heart of glass regulates the concentric growth of the heart in zebrafish. Curr. Biol. *13*, 2138–2147.

Mandel, E.M., Kaltenbrun, E., Callis, T.E., Zeng, X.X., Marques, S.R., Yelon, D., Wang, D.Z., and Conlon, F.L. (2010). The BMP pathway acts to directly regulate Tbx20 in the developing heart. Development *137*, 1919–1929.

Moorman, A.F., Houweling, A.C., de Boer, P.A., and Christoffels, V.M. (2001). Sensitive nonradioactive detection of mRNA in tissue sections: novel application of the whole-mount in situ hybridization protocol. J. Histochem. Cytochem. *49*, 1–8.

Mungrue, I.N., Zhao, P., Yao, Y., Meng, H., Rau, C., Havel, J.V., Gorgels, T.G., Bergen, A.A., MacLellan, W.R., Drake, T.A., et al. (2011). Abcc6 deficiency causes increased infarct size and apoptosis in a mouse cardiac ischemia-reperfusion model. Arterioscler. Thromb. Vasc. Biol. *31*, 2806–2812.

Pachori, A.S., Custer, L., Hansen, D., Clapp, S., Kemppa, E., and Klingensmith, J. (2010). Bone morphogenetic protein 4 mediates myocardial ischemic injury through JNK-dependent signaling pathway. J. Mol. Cell Cardiol. *48*, 1255–1265.

Parinov, S., Kondrichin, I., Korzh, V., and Emelyanov, A. (2004). Tol2 transposon-mediated enhancer trap to identify developmentally regulated zebrafish genes in vivo. Dev. Dyn. *231*, 449–459.

Perner, B., Englert, C., and Bollig, F. (2007). The Wilms tumor genes wt1a and wt1b control different steps during formation of the zebrafish pronephros. Dev. Biol. *309*, 87–96.

Poss, K.D., Wilson, L.G., and Keating, M.T. (2002). Heart regeneration in zebrafish. Science *298*, 2188–2190.

Prabhu, S., Ignatova, A., Park, S.T., and Sun, X.H. (1997). Regulation of the expression of cyclin-dependent kinase inhibitor p21 by E2A and Id proteins. Mol. Cell. Biol. *17*, 5888–5896.

R Core Team. (2013). R: A Language and Environment for Statistical Computing (R Foundation for Statistical Computing).

Sallin, P., de Preux Charles, A.S., Duruz, V., Pfefferli, C., and Jazwinska, A. (2015). A dual epimorphic and compensatory mode of heart regeneration in zebrafish. Dev. Biol. *399*, 27–40.

Schnabel, K., Wu, C.C., Kurth, T., and Weidinger, G. (2011). Regeneration of cryoinjury induced necrotic heart lesions in zebrafish is associated with epicardial activation and cardiomyocyte proliferation. PLoS One *6*, e18503.

Schneider, C.A., Rasband, W.S., and Eliceiri, K.W. (2012). NIH Image to ImageJ: 25 years of image analysis. Nat. Methods *9*, 671–675.

Senyo, S.E., Steinhauser, M.L., Pizzimenti, C.L., Yang, V.K., Cai, L., Wang, M., Wu, T.D., Guerquin-Kern, J.L., Lechene, C.P., and Lee, R.T. (2013). Mammalian heart renewal by pre-existing cardiomyocytes. Nature *493*, 433–436.

Sergeeva, I.A., Hooijkaas, I.B., Van Der Made, I., Jong, W.M., Creemers, E.E., and Christoffels, V.M. (2014). A transgenic mouse model for the simultaneous monitoring of ANF and BNP gene activity during heart development and disease. Cardiovasc. Res. *101*, 78–86.

Shih, Y.H., Zhang, Y., Ding, Y., Ross, C.A., Li, H., Olson, T.M., and Xu, X. (2015). The cardiac transcriptome and dilated cardiomyopathy genes in zebrafish. Circ. Cardiovasc. Genet. *8*, 261–269.

Sleep, E., Boue, S., Jopling, C., Raya, M., Raya, A., and Izpisua Belmonte, J.C. (2010). Transcriptomics approach to investigate zebrafish heart regeneration. J. Cardiovasc. Med. (Hagerstown) *11*, 369–380.

Smith, K.A., Noel, E., Thurlings, I., Rehmann, H., Chocron, S., and Bakkers, J. (2011). BMP and nodal independently regulate lefty1 expression to maintain unilateral nodal activity during left-right axis specification in zebrafish. PLoS Genet. *7*, e1002289.

Sun, B., Huo, R., Sheng, Y., Li, Y., Xie, X., Chen, C., Liu, H.B., Li, N., Li, C.B., Guo, W.T., et al. (2013). Bone morphogenetic protein-4 mediates cardiac hypertrophy, apoptosis, and fibrosis in experimentally pathological cardiac hypertrophy. Hypertension *61*, 352–360.

Szibor, M., Poling, J., Warnecke, H., Kubin, T., and Braun, T. (2014). Remodeling and dedifferentiation of adult cardiomyocytes during disease and regeneration. Cell. Mol. Life. Sci. *71*, 1907–1916.

van Wijk, B., Moorman, A.F., and van den Hoff, M.J. (2007). Role of bone morphogenetic proteins in cardiac differentiation. Cardiovasc. Res. *74*, 244–255.

Wang, J., Panakova, D., Kikuchi, K., Holdway, J.E., Gemberling, M., Burris, J.S., Singh, S.P., Dickson, A.L., Lin, Y.F., Sabeh, M.K., et al. (2011). The regenerative capacity of zebrafish reverses cardiac failure caused by genetic cardiomyocyte depletion. Development *138*, 3421–3430.

Wills, A.A., Holdway, J.E., Major, R.J., and Poss, K.D. (2008). Regulated addition of new myocardial and epicardial cells fosters homeostatic cardiac growth and maintenance in adult zebrafish. Development *135*, 183–192.

Ying, Q.L., Nichols, J., Chambers, I., and Smith, A. (2003). BMP induction of Id proteins suppresses differentiation and sustains embryonic stem cell self-renewal in collaboration with STAT3. Cell *115*, 281–292.

Zaidi, S.H., Huang, Q., Momen, A., Riazi, A., and Husain, M. (2010). Growth differentiation factor 5 regulates cardiac repair after myocardial infarction. J. Am. Coll. Cardiol. *55*, 135–143.

Zimmerman, L.B., De Jesus-Escobar, J.M., and Harland, R.M. (1996). The Spemann organizer signal noggin binds and inactivates bone morphogenetic protein 4. Cell *86*, 599–606.